Charge-Exchange Cross Section of 175- to 250-Mev K^+ in Carbon, Copper, Tungsten, and Nuclear Emulsion*

MARIAN N. WHITEHEAD, ROBERT E. LANOU, JR., VICTOR COOK, JR., AND ROBERT W. BIRGE
Lawrence Radiation Laboratory, University of California, Berkeley, California

(Received October 19, 1959)

The disappearance and presumed charge exchange of K^+ mesons has previously been observed in nuclear emulsions. We have measured the charge-exchange cross section for K^+ energies between 150 and 250 Mev in C, Cu, W, and, as a check, in nuclear emulsion. In addition, a scintillation-counter array was used to detect the charged decay mode of the short-lived K_1^0 produced in the charge-exchange reaction. The measured mean free path in nuclear emulsion is 195 ± 25 cm at 200 Mev. The average corrected free-neutron cross section deduced from the pure elements is 5.9 ± 0.4 mb.

From K^+ charge exchange, and assuming a branching ratio of $\frac{1}{3}$ for decay into the $2\pi^0$ mode compared to all decays for the K_1^0 state, we find a K_1^0/K_2^0 ratio consistent with unity.

I. INTRODUCTION

THE disappearance of K^+-meson tracks in emulsion has been attributed to the reaction $K^++p\rightarrow K^0+n$. According to the predictions of Gell-Mann and Pais,[1] the K^0 is a superposition of two states, the short-lived K_1^0 and the long-lived K_2^0. The K_1^0 in turn has two decay modes,

$$K_1^0\rightarrow\pi^++\pi^-,\quad K_1^0\rightarrow\pi^0+\pi^0.$$

The fraction of K_1^0 going into the $2\pi^0$ mode has been measured to be 0.36.[2] The pure $\Delta I=\frac{1}{2}$ rule predicts 0.33.[1] In a previous paper,[3] we reported the observation of the charged-decay mode of K_1^0 from the charge exchange of 40- to 165-Mev K^+ in the carbon contained in the propane bubble chamber of the Lawrence Radiation Laboratory. From the observed number of events in this experiment we computed a total charge-exchange cross section of 0.6 ± 0.6 mb per carbon neutron. The number from emulsion data[4] is 1.3 ± 0.3 mb per average neutron for the total charge-exchange cross section. These numbers left an uncertainty as to whether the rate of appearance of the K_1^0 charged decay mode was compatible with the Gell-Mann prediction.

Accordingly, a counter experiment was designed to measure both the charge-exchange cross section and the number of K_1^0 decays. An emulsion target was used as a cross calibration, and then the cross sections were measured for carbon, copper, and tungsten at 240- and 175-Mev average K^+-meson energy.

* This work was done under the auspices of the U. S. Atomic Energy Commission.

[1] M. Gell-Mann and A. Pais, *Proceedings of the Glasgow Conference on Nuclear and Meson Physics, 1954* (Pergamon Press, New York, 1954), pp. 342–352.

[2] F. S. Crawford, M. Cresti, R. L. Douglass, M. L. Good, G. R. Kalbfleish, M. L. Stevenson, and H. K. Ticho, Phys. Rev. Letters **2**, 266 (1959).

[3] M. N. Whitehead, R. E. Lanou, R. W. Birge, W. M. Powell, and W. B. Fowler, University of California Radiation Laboratory Report UCRL-8846, July 29, 1959 (unpublished).

[4] R. H. Dalitz, *Reports on Progress in Physics* (The Physical Society, London, 1957), Vol. 20, p. 163. A complete list of references to the original papers is given here.

II. METHOD

A. General Description

An identified beam of K^+ mesons[5] passed through a defining counter and entered a target surrounded by anticounters as shown in Fig. 1. A charge-exchange event was defined as one in which an identified K^+ meson entered the target with none of the anticounters counting. Charge exchanges leading to K_2^0 (long-lived) mesons should be detected with 100% efficiency, whereas with a target of finite size some of the K_1^0 (short-lived) mesons will decay in the target and count in the anticounters. These events are not counted as charge exchanges, and the final data is corrected for this loss.

Besides the decay of the K_1^0, there are several other factors that are critical in the design of the target. A K_2^0-type event can be simulated by an inelastically scattered K^+ which stops in the target in a position such that the charged decay products also stop. Similarly, the backward decay of K^+ mesons in flight which give low-energy decay particles can have the same result. In order to minimize these effects the stopping

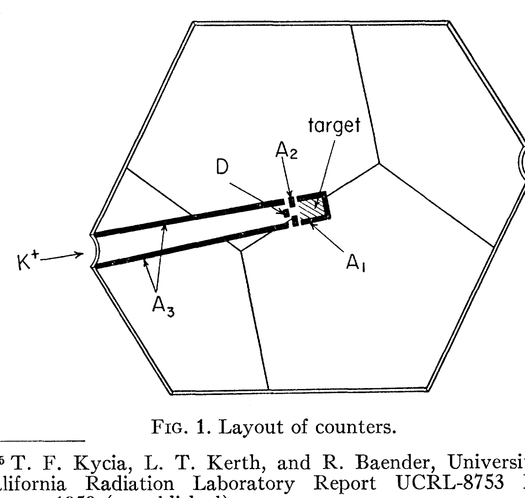

FIG. 1. Layout of counters.

[5] T. F. Kycia, L. T. Kerth, and R. Baender, University of California Radiation Laboratory Report UCRL-8753 Rev., August, 1959 (unpublished).

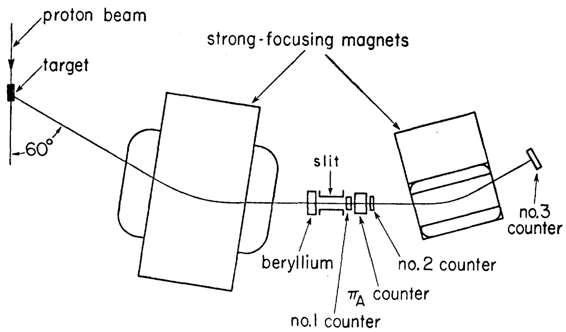

FIG. 2. Diagram of K^+ beam.

power of the target must be small in all dimensions. However, in the charge-exchange process an energetic proton may be ejected from the nucleus. If this proton enters the anticounters an event may be lost. Therefore, the low-density targets used were surrounded by a brass cylinder to keep this correction small.

The detection of the K_1^0 is based on the fact that there is a finite minimum opening angle between the two decay pions which increases as the K_1^0 energy decreases. If the target assembly is surrounded by counters, each of which subtends an angle at the target smaller than this minimum angle, then two counters should count in coincidence when a K_1^0 decays. For 250-Mev K^0 mesons this angle is 72 deg, which allows the entire solid angle to be made up of twelve pentagons fitting together as a dodecahedron. The distance to the counters must be large compared to the mean distance for decay of the K_1^0. These various parameters determined that the dimensions of each pentagon be about 18 in. across and the target about 1 in. in diameter.

B. The Beam

A diagram of the beam trajectory is shown in Fig. 2. It consists of bending magnets, H and C, that had strong-focusing poles serving to focus, as well as momentum-analyze the beam. Small quadrupole lenses Q_1 and Q_2 made fine adjustment possible when the beam energy was changed. A momentum bite of $\pm 2\%$ was taken at the first focus with a slit in a lead collimator, and the beam was then refocused both in momentum and position on the charge-exchange target. The K^+ mesons were identified by coincidence among the time-of-flight counters 1, 2, and 3 and an anticoincidence with a water Čerenkov counter that counted only π mesons. The beam was partially purified by putting an absorber at the first focus that degraded the K momentum more than that of the pions. The difficult process of alignment and testing of this beam had been done already,[5] hence we had merely to add and test the charge-exchange assembly.

The limits on the pion and proton contamination had to be somewhat lower than in the K^+ scattering experiment. Therefore, we added more absorber at the first focus, which increased the momentum difference between the pions and K's with the result that the physical separation was greater between them after the second bending. The following checks were made to measure the beam composition. First, the time-of-flight counters were timed for pions, and the ratio of counting rates with the pion anticounter off and on was measured. This ratio was about 1000, indicating that the anticounter was very effective. Second, the same ratio of counting rates was determined with the time of flight set for K mesons. Here the ratio was 1.36. Thus the K/π ratio of the K peak is 1/0.36 without the pion anticounter, and $(1/0.36)\times 10^3 = 2800$ with the pion anticounter turned on. When the counters were timed for protons, the counting rate was down at least a factor of 400 from that at the K peak, indicating few, if any, protons. If these were all K's getting through the coincidence circuit out of time, then one can assume that the proton contamination in the K peak must also be down by 400 from the counting rate at the proton peak. Thus in the K peak the proton contamination is less than $1/(400)^2 = 0.6\times 10^{-5}$. However, this is not the only source of proton contamination. Interactions of K mesons in the counters can lead to slow protons that could stop in the target, simulating charge-exchange events. These counts must be eliminated. To do so we arranged to measure the pulse height in the defining counter (de) just at the entrance to the charge-exchange target. Stopping protons could then be easily identified. Another use of the pulse-height information was to identify backward decays or inelastic scatters of K^+ in the target which reentered the defining counter, thereby doubling the pulse height. The pulse-height calibration was made at regular intervals during the experiment by turning off the electronic anticoincidence and triggering on K^+ for a few hundred pulses. The beam intensity was such that when the Bevatron and our equipment were operating properly, about five K mesons came down the channel per 10^{10} circulating protons.

C. Counters

Surrounding the cylindrical target was a scintillator in the form of a tube capped at one end (see Fig. 1) and viewed with a light pipe on one side. This cup, labelled A_1 in Fig. 3, was the primary anticounter. A ring anticounter, A_2, immediately in front covered the

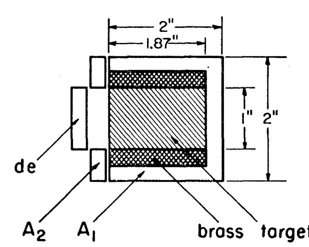

FIG. 3. Target and anticounters.

TABLE I. Description of targets.

	Diameter (cm)	Length (cm)	Surface density (g cm^{-2})
Emulsion	2.78	4.76	18.08
Carbon	2.86	4.72	8.04
Copper	3.86	2.75	2.37
Tungsten	3.12	1.28	24.34
CH_2[a]	2.86	4.76	4.39

[a] Used for carbon at 250 Mev.

annular ring between the center area defined by the defining counter (*de*) and the A_1 anticup. In addition, we surrounded the incoming beam with a tapered cylinder of scintillator (labelled A_3 in Fig. 1) in the event that the pulse-height discrimination in the defining counter did not eliminate back scatters. The A_1 counter was in electronic anticoincidence with a coincidence between an identified K^+ and a pulse from *de*. This anticoincidence pulse triggered two oscilloscope sweeps on which were displayed the pulses from all the counters, including the 12 pentagons. These sweeps were photographed for later inspection. Each of the pulses was first put in coincidence with the output of the K charge-exchange identification circuit, then they were added together with 50-mμsec delay lines before going to the oscilloscope. In this way many spurious background pulses were removed, even though the sweep time was 5 μsec.

Prior to the run, particles were sent through the anticoincidence cup in various orientations and a pulse-height distribution was plotted to prove that the cup would count under all circumstances.

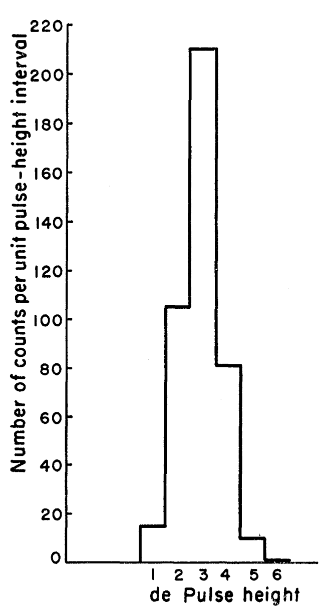

FIG. 4. Defining counter pulse-height distribution.

D. Targets

The dimensions and materials of the various targets are given in Table I.

III. EXPERIMENTAL PROCEDURE

A. Data Analysis

Several different targets were used at incident K^+ energies varying from 175 to 250 Mev. Three types of data were taken for each target at each energy: (a) target in; (2) target out; (c) accidentals with target in. The various densities and stopping powers of the targets made it necessary to have the geometry of each unique, and therefore the "empty" target contained different target holders in each case. The "accidental" runs were made by delaying the K^+ charge-exchange pulse into the oscilloscope coincidence circuit by 40×10^{-8} sec. The three categories were run alternatively several times to average out changes in beam conditions and counter alignment.

In scanning the photographs of the oscilloscope traces, the pulse height of each counter output was measured. Two calibration corrections were then applied before setting acceptable limits. First, the pulse-height distribution in the "*de*" counter was measured when the oscilloscope sweep was triggered on through K's. This distribution for $T_K=250$ Mev is shown in Fig. 4. The acceptable limits were set from 2 to 4 inclusive leaving approximately 3% of the pulses outside. The final cross sections were increased by this percentage. Secondly, a pulse from the charge-exchange trigger was allowed to feed through one channel of the scope coincidence circuit to give a time marker and a definite pulse height, thus calibrating the output amplifier. The average "*de*" pulse height from run to run was then normalized by this calibration and, in addition, all the pentagon and anticounter pulses were so normalized. No limitation was placed on the normalized pulse heights in the anticounters. These counters must be sensitive to a K^+ that stops in the target and then decays; a delayed pulse will be smaller than a prompt one.

Any normalized pulse height greater than two was accepted for the pentagons. The maximum value was

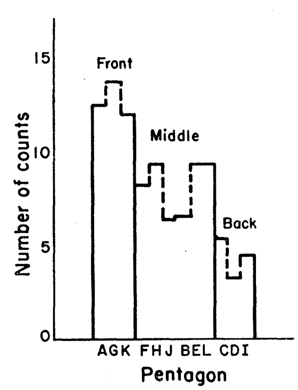

FIG. 5. Pentagon counting rates.

TABLE II. Distribution of counts in various categories.

Target material and K^+ energies (Mev)	N_{1T}	N_{1E}	N_z	A	N_f	N_{2T}	N_{2E}	$d+s$	K_E	f_{mE}	K	f_m
Tungsten												
230	34	1	21	89	1	231	41	5.9×10^{-4}	$10.9\ \times10^4$	0.98	2.29×10^4	0.87
179	32	0	51	170	3	211	4	7.7×10^{-4}	0.852×10^4	0.96	2.04×10^4	0.97
Copper												
179	26	0	44	76	3	164	4	$21\ \times10^{-4}$	$1.05\ \times10^4$	1	1.23×10^4	0.96
Carbon												
239	41	1	42	103	3	394	69	2.4×10^{-4}	$11.4\ \times10^4$	0.95	$16.3\ \times10^4$	0.88
188	24	6	73	225	4	192	29	4.9×10^{-4}	$3.73\ \times10^4$	0.97	3.98×10^4	0.99
151	5	1	58	129	5	43	9	5.1×10^{-4}	$1.91\ \times10^4$	1	1.30×10^4	1
Emulsion												
234	48	1	71	195	4	444	69	11.4×10^{-4}	$11.4\ \times10^4$	0.95	4.59×10^4	0.96
179	35	6	55	189	5	242	29	13.7×10^{-4}	$3.73\ \times10^4$	0.97	2.09×10^4	0.94

limited electronically to seven to preclude feed-through problems. In order to check the relative efficiency of the pentagons, a plot was made of the number of times each pentagon counted a K_1^0 throughout the whole experiment. This is shown in Fig. 5. Counters *AGK*, *FHJ*, *BEL*, and *CDI* are in positions of cylindrical symmetry.

From the recorded data, the K_1^0 and K_2^0 events were selected on the following basis. The K_2^0 category included all events where there were (a) no pentagons and no anticounts, (b) no pentagons and A_3, and (c) one pentagon and no anticounts. The total is called N_2. Categories (b) and (c) were included under the assumption that the pulses were accidentals, thereby making the accidental correction statistically much better. Category (c) includes the small fraction of K_1^0's that decay outside the cup and have one prong that goes out the entrance or exit opening of the dodecahedron.

The K_1^0 category included all events where no anticounter and two or more pentagons counted. The total is called N_1.

On the accidental film the same categories were used, only in this case the *de* pulse height was required to be zero.

After the various categories were selected, the data were reduced in the following manner: The rate for a given type of event (i) per K^+ hitting a particular target is $n_i=N_i/f_mK$ where K is the total number of K^+ hitting the target while N_i events are being registered on the film, and f_m is a correction factor to K equal to the fraction of useable oscilloscope sweeps.

The accidental rates (r_z and r_f) are calculated per charge-exchange trigger. There are two accidental corrections: The first corrects for events lost because accidental pulses appear on the film from the anticounters. The rate is

$$r_z=N_z/A, \tag{1}$$

where N_z is the total accidental sweeps with any anticounter excepting A_3, and A is the total number of oscilloscope sweeps in an accidental run. The second corrects for the appearance of two pentagon events on the accidental runs, i.e., cases of false K_1^0. This rate is

$$r_f=N_f/A, \tag{2}$$

where N_f is the number of accidental sweeps with no anticounter and two or more pentagons.

We can now write for the corrected counting rate of K_2^0 mesons from a given target:

$$n'(K_2^0)=\frac{n_{2T}-n_{2E}-(d+s)-f_2n'(k_1^0)}{1-r_z}, \tag{3}$$

where n_{2T} and n_{2E} are the K_2^0 rates for the target in and out; d and s are corrections for K^+ mesons that decay, at rest after a scatter or in flight, into secondaries that stop *in* the target; and f_2 is the fraction of the K_1^0 mesons that send one prong through a hole in the dodecahedron (3% of surface area is not covered by scintillator) and would be counted as K_2^0's.

The corrected counting rate for K_1^0 is then

$$n'(K_1^0)=\frac{n_{1T}-n_{1E}-r_fn'(k_2^0)}{(1-r_z-f_2)}. \tag{4}$$

The actual number of counts obtained in the various categories are given in Table II and the corrected charge-exchange counts per incident K^+ are given in Table III.

TABLE III. Corrected charge-exchange counts per incident K^+.

Target material and K^+ energies (Mev)	$n'(K_1^0)$	$n'(K_2^0)$
Tungsten		
230	$(2.24\pm0.47)\times10^{-3}$	$(1.29\pm0.11)\times10^{-2}$
179	$(2.22\pm0.50)\times10^{-3}$	$(1.24\pm0.12)\times10^{-2}$
Copper		
179	$(2.87\pm0.69)\times10^{-3}$	$(1.46\pm0.16)\times10^{-2}$
Carbon		
239	$(0.38\pm0.13)\times10^{-3}$	$(0.26\pm0.02)\times10^{-2}$
188	$(0.59\pm0.24)\times10^{-3}$	$(0.47\pm0.06)\times10^{-2}$
151	$(0.43\pm0.35)\times10^{-3}$	$(0.32\pm0.06)\times10^{-2}$
Emulsion		
234	$(1.50\pm0.34)\times10^{-3}$	$(1.13\pm0.09)\times10^{-2}$
179	$(1.97\pm0.62)\times10^{-3}$	$(1.34\pm0.12)\times10^{-2}$

B. Computation of the Production Rates from Observed Rates $n(K_1^0)$ and $n'(K_2^0)$

The true production rates $N(K_1^0)$ and $N(K_2^0)$ are deduced from the corrected counting rates $n'(K_1^0)$ and $n'(K_2^0)$ by the use of the following formulas:

$$N(K_1^0)=\frac{n'(K_1^0)}{(1-f_P)f_E(1-f_B)}, \quad (5)$$

$$N(K_2^0)=\frac{n'(K_2^0)}{(1-f_P)[1+f_Ef_BN(K_1^0)/N(K_2^0)]}. \quad (6)$$

The symbols are explained below.

To see how these formulas are derived, consider first the rate $N(K_1^0)$. The experimentally measured rate, $n'(K_1^0)$, must be corrected for those events which are missed because one or both of the K_1^0 decay products pass through the anticounter, A_1. This may happen either when the particle decays within the target or when it decays outside A_1 but manages to send one of its products backwards into A_1. The fraction of all K_1^0 remaining to be counted, f_E, may be calculated in a straightforward way for each target and energy because the K_1^0 lifetime and the target geometry are well-known quantities. The magnitude of f_E varies from 0.21 in the case of carbon at 175 Mev to 0.51 for tungsten at 250 Mev and is shown in Table IV. The method of computation of f_E is outlined in Appendix I.

The next correction to the $n'(K_1^0)$ rate arises because some events are not counted when an energetic proton manages to escape from the target and trigger A_1. The fraction of events lost by this mechanism is called f_P. The range of values of f_P are from 0.013 for tungsten to 0.084 for carbon and are shown in Table IV. The method of determining f_P is described in Appendix II.

Lastly, compensation must be made for those K_1^0's which decay by the $2\pi^0$ mode outside the target and hence are not counted by double coincidence in the dodecahedron. (Those which decay inside the target succeed in triggering the counter A_1 because of the high probability of converting at least one of the four gamma rays in the target or brass surrounding the target.) The ratio of those K_1^0's decaying by the $2\pi^0$ mode to those decaying by both modes is taken as $\frac{1}{3}$ and designated by the symbol f_B.[2] These three quantities are combined to yield the corrected rate shown in Eq. (5).

Consider now the derivation of the $N(K_2^0)$ rate. Here, as in the $N(K_1^0)$ rate, some events are lost because an energetic proton produced in the nuclear interaction escapes from the target and triggers A_1. The fraction lost is again f_P.

The other correction which must be made to $n'(K_2^0)$ arises because those K^0's which decay outside of the target by the $2\pi^0$ mode of K_1^0 give an electronic identification identical to that of K_2^0 and must, therefore, be removed from the $n'(K_2^0)$ rate. The fraction of events that must be removed is then $f_Ef_BN(K_1^0)/N(K_2^0)$. This correction amounts to about 10%.

The $N(K_1^0)$ and $N(K_2^0)$ rates may then be obtained from Eqs. (5) and (6) and the individual cross sections for charge exchange into the K_1^0 channel, $\sigma(K_1^0)$, and into the K_2^0 channel, $\sigma(K_2^0)$, are directly calculable from

$$\sigma_u(K_1^0)=N(K_1^0)/\rho_T, \quad (7)$$

and

$$\sigma_u(K_2^0)=N(K_2^0)/\rho_T, \quad (8)$$

where ρ is the number of neutrons per square centimeter in the target, T, under consideration.

These cross-sections are called the "uncorrected cross section per neutron" $[\sigma_u=\sigma_u(K_1^0)+\sigma_u(K_2^0)]$ and are tabulated in column 1 of Table V. For emulsion, these uncorrected cross sections correspond to mean free paths of 225±25 cm at 234 Mev and 164±23 cm at 179 Mev.

TABLE IV. Correction factors for production rates and free-neutron cross sections.

Target materials and K^+ energies (Mev)	f_E		f_P	f_c	f_x		f_{sd}
	Peaked	Uniform			Peaked	Uniform	
Tungsten							
230	0.40	0.33	0.013	1.06	1.02	1.01	2.08
179	0.25	0.26	0.013	1.08	1.03	1.01	2.08
Copper							
179	0.30	0.28	0.029	1.05	1.05	1.03	1.78
Carbon							
239	0.27	0.24	0.084	1.01	1.22	1.06	1.34
188	0.22	0.20	0.084	1.01	1.30	1.09	1.34
151	0.20	0.19	0.084	1.01	1.39	1.11	1.34
Emulsion							
234	0.25	0.22					
179	0.21	0.19					

IV. RESULTS

A. Estimation of Free-Neutron Cross Section and $R(K_1^0)/(K_2^0)$

When the neutron involved in the charge exchange is bound in the nucleus instead of being free, there are several effects which make the measured charge-exchange cross section per neutron, σ_u, different from that of the free neutron, σ_N. The effects considered here are the diminution of the cross section by the Coulomb repulsion of the incident K^+ by the positively-charged nucleus, by shielding from the other nucleons in the nucleus, by suppression of charge exchange at forward angles due to the Pauli principle resulting from the endothermic nature of the process, and lastly, the overestimation of the single-collision cross section because occasionally double collisions occur. The details of the computation of these effects are contained in Appendixes 3 to 6. The shielding and double scattering are combined into $f_{sd}(K_1^0)$ and $f_{sd}(K_2^0)$. The shielding

TABLE V. Uncorrected cross sections (σ_u) for K^+ charge exchange, free neutron cross sections (σ_N), and the branching ratio, R, for production of the K_1^0 and K_2^0. Shown are results for two assumed angular distributions and weighted averages.

Target material and K^+ energies (Mev)	σ_u (mb/neutron) Peaked	σ_u (mb/neutron) Uniform	$\sigma_N(K_1^0)$ (mb/neutron) Peaked	$\sigma_N(K_1^0)$ (mb/neutron) Uniform	$\sigma_N(K_2^0)$ (mb/neutron) Peaked	$\sigma_N(K_2^0)$ (mb/neutron) Uniform	σ_N (mb/neutron) Peaked	σ_N (mb/neutron) Uniform	$R(K_1^0/K_2^0)$ Peaked	$R(K_1^0/K_2^0)$ Uniform
Tungsten										
230	2.26	2.49	2.17	2.59	2.77	2.79	4.94±0.49	5.38±0.56	0.78±0.20	0.93±0.22
179	2.78	2.77	3.52	3.94	2.81	2.81	6.33±0.72	6.75±0.82	1.25±0.31	1.40±0.34
Copper										
179	3.59	3.74	3.67	3.85	3.24	3.21	6.91±0.89	7.06±0.93	1.13±0.30	1.19±0.31
Carbon										
239	4.18	4.45	3.37	3.31	3.38	2.97	6.75±1.11	6.28±1.09	1.00±0.28	1.11±0.38
188	3.78	3.97	3.18	2.66	3.33	2.81	6.51±1.29	5.47±1.21	0.95±0.41	0.95±0.46
151	2.80	2.87	2.74	2.30	2.43	1.94	5.17±2.25	4.24±1.90	1.12±0.98	1.18±1.0
Emulsion										
234	3.54±0.38	3.78±0.41							0.86±0.22	0.97±0.24
179	4.84±0.78	5.13±0.82							1.12±0.33	1.23±0.34
			Weighted average				5.79±0.34	5.97±0.41	0.96±0.09	1.08±0.09

and double-scattering factors have different values for K_1^0 and K_2^0 rates because multiple collisions involve loss of energy for the K^+ meson leading to appreciably more decays of the K_1^0 in the target, whereas the K_2^0 rate is not affected. The $\sigma_N(K_{1,2}^0)$ are the cross sections per free neutron for K_1^0 or K_2^0 obtained from the $\sigma_u(K_{1,2}^0)$ by the formula

$$\sigma_N(K_i^0)=f_cf_xf_{sd}(K_i^0)\sigma_u(K_i^0) \tag{9}$$

where $i=1$, 2, and the total corrected cross section per neutron by

$$\sigma_N=\sigma_N(K_1^0)+\sigma_N(K_2^0). \tag{10}$$

In general the combined factor $f_cf_xf_{sd}$ amount to increasing σ_u by about a factor of two. The individual factors are tabulated in columns 3 to 5 of Table IV and the resulting free-neutron cross sections in Table V. The weighted average of the free-neutron cross section for all elements is also given.

B. Estimate of Phase Shift

An estimate of the phase shift for the zero-isospin, zero-orbital angular-momentum partial wave can be made from the measured charge-exchange cross sections. We denote the amplitude for each partial wave state by a_{mn}, where the first subscript refers to the isospin and the second subscript is 0, 1, 3 for the S, $P_{\frac{1}{2}}$, and $P_{\frac{3}{2}}$ angular momentum. The differential cross section for K^+ interactions may be written as

$$d\sigma/d\Omega=\lambda\!\!\!^{-}(A+B\cos\theta+C\cos^2\theta), \tag{11}$$

and the total cross sections as

$$\sigma=4\pi\lambda\!\!\!^{-2}(A+\tfrac{1}{3}C), \tag{12}$$

where, for the reaction $K^++P\rightarrow K^++P$, we have

$$A_{+P}=(a_{10})^2+(a_{11}-a_{13})^2, \tag{13}$$

$$B_{+P}=2\,\mathrm{Re}(a_{10})^*(2a_{11}-a_{13}), \tag{14}$$

and

$$C_{+P}=3(a_{11})^2+6\,\mathrm{Re}(a_{11})^*a_{13}. \tag{15}$$

Similarly, for the neutron reactions we have

$$A_{+N}=\tfrac{1}{4}(a_{10}\pm a_{00})^2+\tfrac{1}{4}[(a_{11}-a_{13})\pm(a_{03}-a_{01})]^2, \tag{16}$$

$$B_{+N}=\tfrac{1}{2}\,\mathrm{Re}(a_{10}\pm a_{00})^*[(2a_{13}+a_{11})\pm(2a_{03}+a_{01})], \tag{17}$$

and

$$C_{+N}=\tfrac{1}{4}[(2a_{13}+a_{11})\pm(2a_{03}+a_{01})]^2-\tfrac{1}{4}[(a_{13}-a_{11})\pm(a_{03}-a_{01})]^2. \tag{18}$$

Where a choice of sign exists, the plus corresponds to the reaction $K^++N\rightarrow K^++N$, and the minus corresponds to $K^++N\rightarrow K^0+P$. Further, the amplitudes, a_{mn}, are related to the phase shifts, δ_{mn}, by

$$a_{mn}=(e^{2i\delta_{mn}}-1)/2i. \tag{19}$$

Experimental measurements of $d\sigma/d\Omega$ for the reaction $K^++P\rightarrow K^++P$ from very low energy up to the energies of this experiment indicate that it is consistent with isotropy.[6] Either a pure S wave or pure $P_{\frac{1}{2}}$ state could give this distribution. If one argues that pure $P_{\frac{1}{2}}$ is the cause at the higher energy and pure S at the lower energy, then the angular distribution at some intermediate energy should show considerable anisotropy due to the presence of these two states. This anisotropy is not observed, and we choose to interpret this persistence of isotropy as due to S-wave interaction only. We, therefore, set $a_{11}=a_{13}=0$. We then use the previously determined value of a_{10},[5] which yields $\delta_{10}=33.4°\pm2.3°$. Under these conditions, we have

$$\sigma_{\mathrm{tot}}(\mathrm{Neutron})=2\sigma_{\mathrm{ex}}(N)+4\pi\lambda\!\!\!^{-2}\,\mathrm{Re}a_{00}^*a_{10}, \tag{20}$$

or

$$\sin\delta_{00}\cos(\delta_{10}-\delta_{00})=\frac{[\sigma_{\mathrm{tot}}(N)-2\sigma_{\mathrm{ex}}(N)]}{4\pi\lambda\!\!\!^{-2}\sin\delta_{10}}, \tag{21}$$

[6] A summary is to be found in the *1958 Annual International Conference on High-Energy Physics at CERN*, edited by B. Ferretti (CERN Scientific Information Service, Geneva, 1958).

where $\sigma_{\text{tot}}(N)$ is the neutron total cross section and $\sigma_{\text{ex}}(N)$ is the neutron charge-exchange cross section. The value of 12+3 mb at 239 Mev is obtained for $\sigma_{\text{tot}}(N)$ by interpolation from the data of Lannutti[7] and Burrowes et al.[8] Under these conditions we find

$$\delta_{00}=2°\pm1\tfrac{3}{2}. \tag{23}$$

The large error is due chiefly to the uncertainty in the interpolated neutron total cross section, the lower limit is cut off at 0 deg to be consistent with the repulsive S-wave interaction as determined from Coulomb interference.[5,6]

C. Determination of $\sigma_{\text{ex}}/\sigma_{\text{In}}$

The ratios of the K^+ charge-exchange cross section to the K^+ total inelastic cross section determined previously were from nuclear-emulsion experiments and hence represent an averaging over several different nuclei.[6,7,9] Because the present experiment directly measures the exchange cross section in pure elements, we combine these results with previously measured total cross sections[10] to determine the ratios for the pure elements C, Cu, and W. For an energy of 200 Mev, the ratios which are in substantial agreement with the most recent compilation of emulsion results[11] are 0.23, 0.30, and 0.34 for carbon, copper, and tungsten, respectively, with an error of ±0.05.

D. The Ratio, $R(K_1^0/K_2^0)$

In the description of the neutral K meson as a particle mixture,[1] the functions for the two decay modes are expressed as

$$|K_2^0\rangle=\frac{p|K^0\rangle+q|K^{-0}\rangle}{[(p^2+q^2)^{\frac{1}{2}}]^{\frac{1}{2}}}, \tag{23}$$

and

$$|K_2^0\rangle=\frac{p|K^0\rangle-q|K^{-0}\rangle}{[(p^2+q^2)^{\frac{1}{2}}]^{\frac{1}{2}}}.$$

The coefficients p and q must be equal to one if time reversal invariance is true. One consequence of $p=q=1$ is that branching ratio $R(K_1^0/K_2^0)$ must also equal one.

Since the cross sections are determined in this experiment from the raw data in terms of two different angular distributions, the ratio R is also determined in terms of these two angular distributions. As is shown in Table V, we obtain $R=0.96\pm0.09$ for the peaked distribution and $R=1.08\pm0.09$ for the uniform distribution. Both values are consistent with the theoretically predicted value of 1. Rather than interpret this result as a check on the invariance of the time-reversal operation, we prefer to assume that the true value is $R\equiv1$ and interpret the near-equality of the measured value to $R=1$ as a check on the internal consistency of the calculated parameters of this experiment. We note that a change in the ratio $2\pi^0/[2\pi^0+(\pi^+\pi^-)]$ of -0.1 changes R from 1.00 to 1.15.

CONCLUSIONS

The mean-free path for K^+ charge exchange in emulsion is in agreement with previously measured values.

The value for the K^+ charge-exchange cross section on a free neutron is of the order of 6 mb in the energy region from 175 to 250 Mev (see Table V). The ratio of the charge-exchange cross section to the inelastic cross section is of the order of 0.3. Both of these results are consistent with an increased interaction in the $T=0$ state, as suggested previously.[4]

Previously no evidence existed as to the identity of the products of the K^+ disappearance in emulsion. If strangeness is conserved in K^+ interactions, then the number of K^0's detected should equal the number of K^+'s that disappear. In this experiment the K^+ disappearance and the fraction of K^0's decaying by the K_1^0 mode are positively electronically detected, and the other mode K_2^0 is assumed to make up the difference (after correction for $2\pi^0$ decay of K_1^0).

If the ratio $R(K_1^0/K_2^0)$ is not equal to one, then either strangeness is not conserved or time-reversal invariance is not true, or both. However our measured value of R is consistent with unity.

ACKNOWLEDGMENTS

The authors are greatly indebted to Dr. Leroy T. Kerth who made available to us the momentum-analyzed beam that made this experiment possible. Our charge-exchange equipment was set up in this beam at the close of his experiment.

In addition, we wish to thank Dr. Thaddeus F. Kycia and Dr. Leroy Kerth and Ralph Baender, Robert P. Matsen, and Gerald L. Schnurmacher for their assistance during the actual running of the experiment. We are also grateful to Mr. Robert Fry, Mrs. Beverly Jerome, and Mrs. Marilynn McLaren for their scanning of the film. Mrs. Marjorie Simmons and Mr. Seymour Singer very kindly wrote the data-handling program for the IBM-650 computer. Fabrication of the intricate counters was done by technicians in the Accelerator Technician Shop under the direction of Mr. Donald Bliss. The success of the experiment depended on their skill and ingenuity. We further wish to thank Dr. Edward J. Lofgren and the crew of the Bevatron for their assistance and for the successful operation of the Bevatron.

[7] J. E. Lannutti, S. Goldhaber, G. Goldhaber, W. W. Chupp, S. Giambuzzi, C. Marchi, G. Quareni, and A. Wataghin, Phys. Rev. **109**, 2121 (1958).

[8] H. C. Burrowes, D. O. Caldwell, D. H. Frisch, D. A. Hill, D. M. Ritson, and R. A. Shluter, Phys. Rev. Letters **2**, 117 (1959).

[9] D. H. Stork (private communication). We are indebted to Dr. Stork for communicating his results to us prior to publication.

[10] L. T. Kerth, T. F. Kycia, and L. Van Rossum, Phys. Rev. **109**, 1784 (1958).

[11] M. Grilli, L. Guerriero, M. Merlin, and G. A. Salandin, Nuovo cimento **10**, 205 (1958).

APPENDIX I. COMPUTATION OF f_E

In order to determine what fraction of real events are lost because of K_1^0 decay products counting in A_1, a Monte Carlo calculation was carried out on an IBM-650 computer. The direction of all incident K^+'s was taken along the target axis and the distribution of charge exchanges was taken to be uniform over the target. The charge exchange was assumed to take place at a point on a single neutron at rest. Energy loss and scattering of the K^+ in the target was neglected. The following parameters were picked at random: (a) a point in the target, (b) a direction of the K_1^0, (c) a distance before decay (weighted according to the mean life), and (d) the barycentric angle for decay of the K_1^0. The half-life was corrected to proper time by assuming an energy of the K_1^0 as if K^+-nucleon elastic scattering had taken place. By the use of an angular distribution of the K_1^0 in the laboratory system, it was possible to compute the total fraction of K_1^0 that would be lost and also the efficiency for escape per $d(\cos\theta_{\text{lab}})$ as a function of $\cos\theta_{\text{lab}}$. These quantities were computed for each target and for each energy. A value of 0.95×10^{-10} sec was used for the mean life of the K_1^0 mode.

For purposes of reducing the data, a center-of-mass (c.m.) angular distribution must be assumed for the resulting K^0 in the exchange process. We have reduced the data in terms of two different distributions. The first is uniform in $d(\cos\theta)$ and the second is of the form $d\sigma/d\Omega=0.168+0.415\cos_{\text{c.m.}}$; this distribution is derived for the exchange process from the results on K^++p and K^++n in emulsion.[9] The K_1^0 escape efficiency for each of these assumed distributions could then be easily found by utilizing the above-mentioned Monte Carlo results. At small angles these distributions are suppressed, as mentioned in Appendix I, because of the necessity of imparting a certain minimum amount of energy to the recoiling proton. This minimum energy is determined by the endothermic nature of the exchange process.

We have also corrected the data for double scattering of the emitted K_1^0 as per Appendix VI leading to the total corrections f_E listed in Table IV.

APPENDIX II. CALCULATION OF f_p

The factor, f_p, which corrects for those events that are lost because energetic recoil protons sometimes escape from the target and count in A_1, depends on the target material. For the emulsion target we use data obtained from emulsion stacks.[7,9] For the other elements we note that the energy in the center of mass of the charge-exchange system is similar to that in some nucleon-nucleon experiments done with the 184-in. cyclotron.[12] The energy and angular distributions of recoil protons were measured from various elements close to those that we used. These distributions were used to compute what fraction of our charge-exchange events would be rejected by integrating over all possible directions in each of the targets. These corrections, f_P, are given in Table IV.

[12] E. Bailey and W. H. Barkas, University of California Radiation Laboratory Report UCRL-3334, March 1, 1956 (unpublished).

APPENDIX III. COULOMB CORRECTION

The correction for the reduction of the effective nucleon radius by the Coulomb distortion of the incident wave[13] was made by increasing the measured cross section by the factor

$$f_c=(1+eV_c/T)^2, \tag{24}$$

where we have the Coulomb interaction energy, $eV_c=e^2Z/R$, and $R=1.2\times10^{-13}A_{\frac{1}{3}}$.

The values f_c used for the various targets and energies are given in Table IV.

APPENDIX IV. NUCLEAR SHIELDING CORRECTIONS

We assume that the ratio of the charge-exchange cross sections for free neutrons to that for bound neutrons is the same as the ratio of the total scattering cross section on free nucleons to that on bound nucleons. We then use the calculations of nuclear transparency by Rossi[14] to evaluate the ratio of the individual scattering cross sections in terms of the transparency factor $(\sigma_i/\pi R^2)$. This factor is a function of the mean free path in nuclear matter l_c) which is calculated from the known free neutron and proton scattering cross sections.

By definition, the transparency factor is

$$\sigma_i/\pi R^2=A\sigma/\pi a_0^2A^{\frac{2}{3}}, \tag{25}$$

where σ is the average measured total cross section per nucleon, A the atomic weight, and $a_0A^{\frac{1}{3}}=R$, the nuclear radius.

Therefore we have

$$\sigma=(\sigma_i/\pi R^2)(\pi a_0^2/A^{\frac{1}{3}}), \tag{26}$$

and the desired ratio is

$$\alpha=\frac{\sigma_f}{\sigma}=\frac{\sigma_f A^{\frac{1}{3}}}{(\sigma_i/\pi R^2)\pi a_0^2}, \tag{27}$$

where σ_f is the average free-nucleon cross section. The mean free path in nuclear matter is

$$l_c=\frac{1}{\sigma_f\rho_{\text{nucl.}}}=\frac{4\pi a_0^3}{3\sigma_f}, \tag{28}$$

$$\sigma_f=\frac{Z\sigma_p+(A-Z)\sigma_n}{A}, \tag{29}$$

[13] M. Blatt and F. Weiskopf, *Theoretical Nuclear Physics* (John Wiley & Sons, Inc., New York, 1952).

[14] Bruno Rossi, *High-Energy Particles* (Prentice-Hall, Inc., New York, 1952), p. 359.

and $\sigma_P = 16$ mb and $\sigma_N = 12$ mb are the values used for total cross sections for K^+ scattering on free protons and free neutrons. The correction factor α, calculated for each element and combined with the double-scattering corrections of Appendix VI appears as f_{sd} in Table V.

APPENDIX V. PAULI EXCLUSION PRINCIPLE CORRECTIONS

Sternheimer[15] calculated the minimum angle θ of the K^+-nucleon scatter within the nucleus in order that the momentum of the recoil nucleon be outside the occupied Fermi distribution, starting with an average value of the Fermi energy T_F. In our case we substituted for T_F the sum of the $K^0 - K^+$ mass difference and of the energy necessary to transform the target nucleus (A,Z) to $(A, Z+1)$. The formula used is

$$\cos\theta_{\min} = 1 - 1.558 T_F / T_1. \tag{30}$$

Here T_1 equals the effective K^+ energy inside the nucleus,

$$T_1 = T_{\text{lab}} - V_c - V_t,$$

where T_{lab} is the laboratory kinetic energy, V_c, the Coulomb potential, is taken to be $Ze/(1.2 \times 10^{-\frac{1}{3}} A^{\frac{1}{3}})$, and V_t, the repulsive K^+ nuclear potential, is taken to be 20 Mev.[15]

The magnitude of the solid-angle correction f_x determined by the cutoff angle $\theta_{\min}$ depends on the angular distribution of the charge exchange on the nucleons. Table V shows the amounts the measured cross sections were increased for two assumed angular distributions mentioned before—spherically symmetric and peaked forward.

[15] R. M. Sternheimer, Phys. Rev. **106**, 1027 (1957).

APPENDIX VI. DOUBLE SCATTERING CORRECTIONS

If a K^+ scatters a second time in the nucleus, it may charge-exchange and increase the number of events over what would be expected from the nuclear shielding calculation. The K^+ energy will be lowered by the first scatter, and consequently the probability of the K_1^0 decaying in the target is increased. The effect of third- and greater-order scatters are ignored. The measured cross section is increased over the actual cross section as follows:

$$\sigma_{\text{meas}} = \sigma_{\text{act}}[1 + (1-j) R P_2 \beta], \tag{31}$$

where $1-j$ is the fraction of K^+ left after first collision $(=0.8)$, R is the ratio of cross sections at the energies of second and first collisions, P_2 is the probability of a second collision, and β is the ratio of escape factors of the K^0 in the first and second collisions.

Let $R=1$, as we have no evidence in this experiment for the change in the cross section; this value will give the maximum possible correction.

TABLE VI. Double scattering correction factors.

Element	$f_d(K_1^0)$	$f_d(K_2^0)$
C	0.94	0.91
Cu	0.91	0.87
W	0.89	0.84

From the probability of any collision, $\sigma_1/\pi R^2$, which is known, P_2 is calculated. For $\sigma_1/\pi R^2 = 1 - e^{-x}$, we have $P_2 = (x^2/2) e^{-x}$. The value of β is 1 for K_2^0 events and 0.68 for K_1^0. If we write $\sigma_{\text{act}} = (\sigma_{\text{meas}}) f_d(K_{1,2}^0)$, we obtain the correction factors $f_d(K_{1,2}^0)$ which are given in Table VI.